Plasmonics (2014) 9:203–207
DOI 10.1007/s11468-013-9613-z

Extraordinary Optical Transmission Property of X-Shaped Plasmonic Nanohole Arrays

Yongkai Wang · Yan Qin · Zhongyue Zhang

Received: 26 May 2013 / Accepted: 21 August 2013 / Published online: 5 September 2013

Abstract Optical transmission properties of periodic X-shaped plasmonic nanohole arrays in a silver film are investigated by performing the finite element method. Obvious peaks appear in the transmission spectra due to surface plasmon polaritons (SPPs) on the top surface of the silver film, to the Fabry–Ferot resonance effect of SPPs in the nanohole, and to the localized surface plasmon resonance of the nanohole. Besides the topologic shape parameters of the X-shaped nanohole, transmission properties strongly depend on incident polarization. The results of this study not only present a tunable plasmonic filter, but also aid in the understanding of the mechanisms of the extraordinary optical transmission phenomenon.

Keywords Extraordinary optical transmission · Plasmonics · Surface plasmon polariton · Localized surface plasmon

Introduction

In 1998, T. W. Ebbesen first studied the optical transmission properties of a periodic subwavelength rectangular hole in a thin metal film and found that light transmission rate is higher than the area ratio of the hole and the film when the aperture is smaller than the incident wavelength. This phenomenon is called extraordinary optical transmission (EOT) [1]. Given the association of the EOT phenomenon with integrated optics [2], highly sensitive biological sensing and detection [3], surface-enhanced Raman scattering [4], and other nonlinear optical effects, EOT in a metal film with holes has gradually become popular topic for research [5–15].

EOT phenomenon is mainly due to the match between the wavelength of surface plasmon polaritons (SPPs) and the period of the aperture array [16]. For the subwavelength hole array inside a metallic film, when the array period matches the wavelength of SPPs excited on the film, strong electron oscillation is excited around the hole. The formed strong electron oscillation between two sides of the hole results in the larger transmittance funneled through the smaller aperture and propagate to the other side of the film. Thus, the localized surface plasmon (LSP) of the subwavelength hole also plays an important role in the EOT phenomenon [17–19]. To better understand the contribution of SPPs and of LSPs to the EOT phenomenon, researchers had fixed the shape and the size of hole and changed the period of the structure [20]. Previous results showed that both LSP and SPP have important roles in the EOT phenomenon and that when they exhibit a similar energy, the hole becomes conductive to transmission. In addition, the hole can be regarded as a Fabry–Ferot resonant nanocavity, with both ends open. When the spread of SPPs in the hole satisfies a certain phase condition, the hole achieves maximum transmittance [21]. Hence, the length of the hole influences EOT.

Recently, researchers have investigated the optical transmission properties of nanoholes with circular [22], spheroid [23], and triangular [24] structures. When the shapes of the nanohole become more complex, novel transmission properties emerge [25–32].

In this paper, we examine optical transmission properties of X-shaped plasmonic nanohole arrays in a silver (Ag) film. Obvious peaks appear in the transmission spectra due to SPPs on the top surface of the film, to the Fabry–Ferot resonance of SPPs in the nanohole, and to LSPs in the nanohole. In addition, we study the effect of topologic shape parameters of the

Y. Wang · Z. Zhang (✉)
School of Physics and Information Technology, Shaanxi Normal University, Xi'an 710062, China
e-mail: zyzhang@snnu.edu.cn

Y. Qin · Z. Zhang
School of Physical Science and Technology, Southwest University, Chongqing 400715, China

X-shaped nanohole and of incident polarization to transmission properties.

Structure and Computational Method

The X-shaped nanohole arrays analyzed in this study are presented in Fig. 1a. The nanoholes are arranged in a rectangular manner in the Ag film. The transverse and the longitudinal periods are a and b, respectively. The thickness of the Ag film is denoted as d. Figure 1b shows the enlarged X-shaped nanohole that has a width of w and a length of 300 nm. The inclined angle of the X-shaped nanohole is fixed at 60°. In the calculations, light irradiates perpendicularly to the film with a polarization angle θ toward the x-direction, as shown in Fig. 1a. The transmission properties of the X-shaped nanohole arrays are numerically investigated by performing the finite element method (COMSOL Multiphysics). The complex relative permittivity of Ag is obtained from [33].

Results and Discussion

Figure 2 plots the simulated transmission spectra of the X-shaped nanohole arrays with different polarization angles θ of 0°, 30°, 60°, and 90° with fixed a=500 nm, b=500 nm, d=200 nm, and w=50 nm. The wavelength of the spectrum ranges from 0.6 to 1.2 μm. When θ=0°, two transmission peaks occur at λ=0.720 μm and λ=0.985 μm, respectively. When θ=30°, four transmission peaks appear at λ=0.675 μm, λ=0.715 μm, λ=0.835 μm, and λ=0.975 μm, respectively. With the increase in θ, transmittances at λ=0.675 μm and λ=0.835 μm increase dramatically. Meanwhile, transmittances at λ=0.715 μm and λ=0.975 μm decrease. At θ=90°, transmittance peaks at approximately λ=0.715 μm and that at λ=0.975 μm disappear, and there are only two peaks in the transmission spectrum. Based on the trends demonstrated by the transmission peaks, we divide the transmission peaks into four groups (modes I, II, III, and IV), as illustrated in Fig. 2.

To investigate the origins of the transmission peaks in Fig. 2, we examined the corresponding steady-state electric field distributions. Figure 3 shows the steady-state electric field distributions of the X-shaped nanohole at θ=60°. a, d, g, and j of Fig. 3 present the electric field distributions on the top surface of the film, and b, e, h, and k exhibit the electric field distributions at the cross sections of the zx plane through the center of the X-shaped nanohole. Lastly, c, f, i, and l of Fig. 3 display the electric field distributions at the cross sections of the yz plane through the center of the X-shaped nanohole. Given that the inclined angle of the X-shaped nanohole in the x-direction is 60°, the width of the hole in the x-direction is smaller than that in the y-direction. a to c in Fig. 3 demonstrates the steady-state electric field distributions at mode I (λ=0.945 μm); in a of Fig. 3, electric field distributions strongly occur around the corners in the x-direction. A comparison between b and c of Fig. 3 shows that electric field distributions are stronger at the opposite sides of the X-shaped nanohole in the x-direction. Therefore, mode I can be attributed to LSP resonance of the X-shaped nanohole with the incident polarization component in the x-direction. Similarly, mode II is attributed to LSP resonance of the X-shaped nanohole with the incident polarization component in the y-direction. As shown in g to i of Fig. 3, at mode III (λ=0.710 μm), electric field distributions strongly occur around the corners of the X-shaped nanohole in the x-direction, similar with that in a. However, at the cross sections of the zx and yz planes, electric field distributions strongly occur at the top and at the bottom surfaces of the nanohole, which are in contrast to those presented in b and c of Fig. 3, respectively. Mode III can be attributed to the resonance of SPPs in the nanohole at incident polarization in the x-direction. Similarly, mode IV is attributed to the resonance of SPPs in the nanohole at incident polarization in the y-direction. Therefore, the origins of modes I, II, III, and IV sufficiently interpret the polarization-dependent transmission spectra of the X-shaped nanohole arrays.

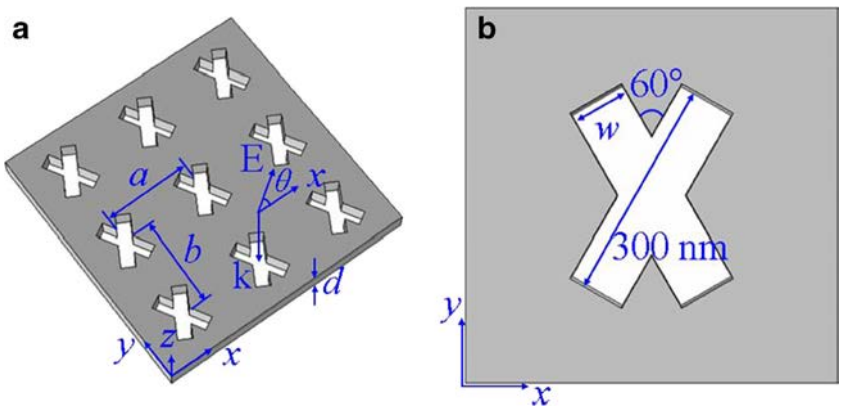

Fig. 1 **a** The proposed X-shaped nanohole arrays and the irradiation condition. **b** Structural parameters of the X-shaped nanohole

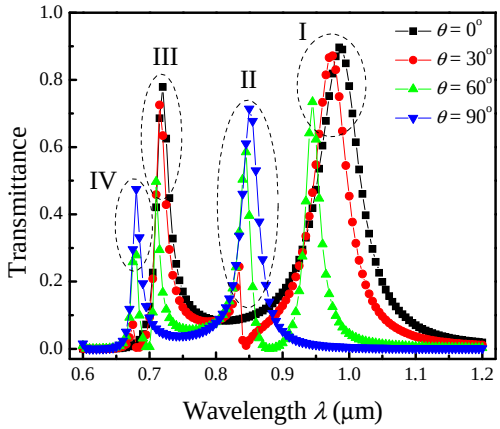

Fig. 2 Calculated transmission spectra of the X-shaped nanohole arrays with different incident polarization angles

To investigate the effect of film thickness d on the transmittance of the X-shaped nanohole arrays, d is increased from $d=160$ nm to $d=240$ nm, with fixed $a=500$ nm, $b=500$ nm, $w=50$ nm, and $\theta=60°$. As shown in Fig. 4, modes I and II are weakly affected by d. However, the wavelengths of modes III and IV red shift dramatically as d increases. Given that modes I and II are attributed to LSP in the X-shaped nanohole at different incident polarizations, the increase of d does not affect LSP. Consequently, transmission peaks do not significantly shift. Given that modes III and IV are attributed to the resonance of SPPs in the nanohole, the increase of d increases the length of the resonator, resulting in the red shift of the resonant wavelengths.

To investigate the influence of the width w of the X-shaped nanohole on the transmittance spectra, w is increased from $w=40$ nm to $w=70$ nm, with fixed $a=500$ nm, $b=500$ nm, $d=200$ nm, and $\theta=60°$. As shown in Fig. 5, the wavelengths of modes I, II, III, and IV blue shift as w increases. Specifically, modes I and II blue shift dramatically from $\lambda=0.985$ μm to $\lambda=0.920$ μm, and from $\lambda=0.905$ μm to $\lambda=0.800$ μm, respectively. However, the wavelengths of modes III and IV

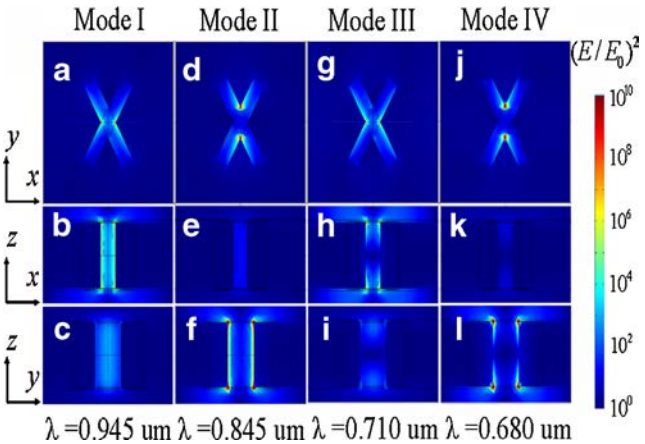

Fig. 3 Steady-state electric field distributions of the X-shaped nanohole at modes I, II, III, and IV at $\theta=60°$

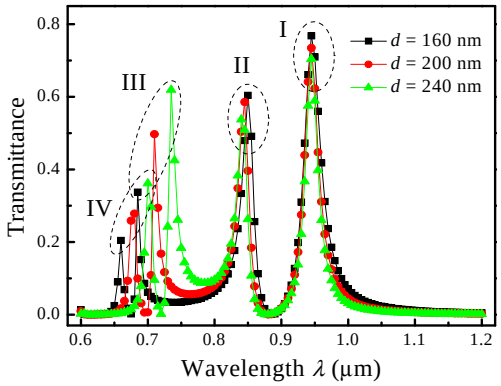

Fig. 4 Calculated transmission spectra of the X-shaped nanohole arrays with different film thickness d

do not significantly shift. As discussed previously, modes I and II are attributed to LSP in the X-shaped nanohole. Therefore, an increase in the width of the X-shaped nanohole will reduce the gap between adjacent nanoholes, resulting in the blue shift of the wavelengths of modes I and II. Meanwhile, an increase in w will decrease the confinement of SPPs in the nanohole, subsequently increasing the wavelength of SPPs in a one specific excitation wavelength. As a result, the resonant modes of modes III and IV blue shift. With the width at the cross section of the yz plane varying faster than that of the zx plane as w increases, the transmission peak of mode IV blue shifts faster than that of mode III.

To investigate the effect of the period to the transmittance spectra, we vary the periods of the X-shaped nanohole arrays in the x- and in the y-directions. Figure 6a shows the simulated transmittance spectra with different transverse periods a in the x-direction, with fixed $b=500$ nm, $d=200$ nm, $w=50$ nm, and $\theta=60°$. Four transmission peaks are observed in the spectra, corresponding to modes I, II, III, and IV. The wavelengths of modes II and IV do not noticeably shift because they correspond to the incident polarization in the y-direction. In contrast, modes I and III are much more sensitive to the period in the x-direction. An increase in the

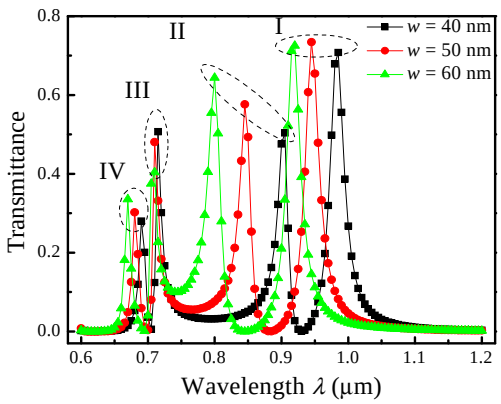

Fig. 5 Calculated transmission spectra of the X-shaped nanohole arrays with different slit width w

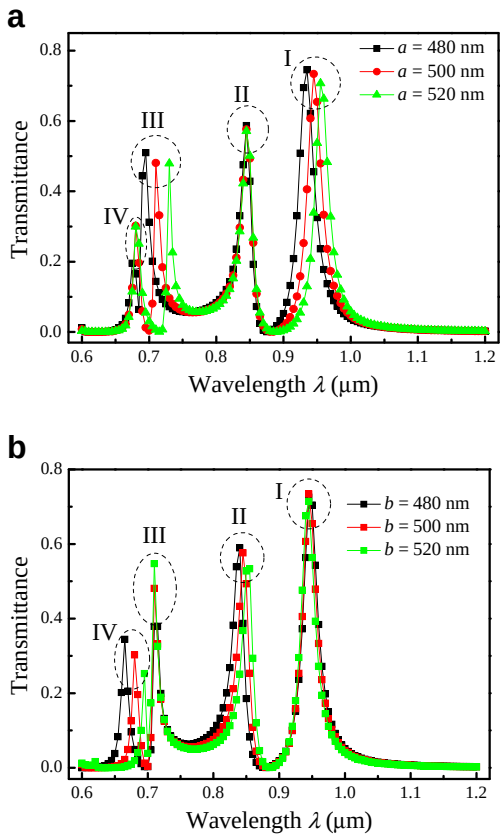

Fig. 6 Calculated transmission spectra of the X-shaped nanohole arrays with **a** different periods in the *x*-direction and **b** different periods in the *y*-direction

transverse period of the X-shaped nanohole by 20 nm results in a red shift of the transmittance peaks by approximately 20 and 40 nm, respectively. Given that mode I is attributed to LSP resonance of the X-shaped nanohole, the increase in a will increase the electron oscillation length on the metal film, resulting in the red shift of the wavelength of mode I. At mode III, SPPs on the top surface are coupled into the nanohole. To achieve maximum transmittance, the period of the nanohole should match the wavelength of SPPs on the top surface of the Ag film. Thus, the wavelengths of mode III red shift as a increases. Figure 6b shows the simulated transmittance spectra with different longitudinal periods b in y-direction, with fixed $a=500$ nm, $d=200$ nm, $w=50$ nm, and $\theta=60°$. Four obvious transmission peaks appear in the spectra. The wavelengths of modes I and III do not shift as b increases. However, the wavelengths of modes II and IV red shift as b increases. These trends are similarly explained with those exhibited in Fig. 6a.

Conclusion

In this paper, transmission properties of periodic X-shaped plasmonic nanohole arrays are studied numerically. Results show that four transmission peaks occur in the transmission spectra of the nanohole arrays due to SPPs on the top surface of the Ag film, to the resonance effect of SPPs in the nanohole, and to LSP in the nanohole. Given that the X-shaped nanohole is anisotropic, its transmission properties are strongly dependent on incident polarizations. In addition, the structural parameters of the X-shaped nanohole and the nanohole array periods strongly affect transmission properties. The results of this study will not only be significant for specific plasmonic applications, but will also be helpful in understanding the mechanisms of the EOT phenomenon.

Acknowledgments This work was supported by the National Natural Foundation of China (grant no. 11004160) and the Fundamental Research Funds for the Central Universities (grant no. GK201303007).

References

1. Ebbesen TW, Lezec HJ, Ghaemi HF, Thio T, Wolff PA (1998) Extraordinary optical transmission through sub-wavelength hole arrays. Nature 391:667–669
2. Barnes WL, Dereux A, Ebbesen TW (2003) Surface plasmon subwavelength optics. Nature 424:824–830
3. Dahlin A, Zach M, Rindzevicius T, Kall M, Sutherland DS, Hook F (2005) Localized surface plasmon resonance sensing of lipid-membrane-mediated biorecognition events. J Am Chem Soc 127: 5043
4. Du LP, Tang DY, Yuan GH, Wei SB, Yuan XC (2013) Emission pattern of surface-enhanced Raman scattering from single nanoparticle-film junction. Appl Phys Lett 102:081117
5. Rindzevicius T, Alaverdyan Y, Dahlin A, Höök F, Sutherland DS, Käll M (2005) Plasmonic sensing characteristics of single nanometric holes. Nano Lett 5:2335–2339
6. Gbur G, Schouten HF, Visser TD (2005) Achieving superresolution in near-field optical data readout systems using surface plasmons. Appl Phys Lett 87:191109
7. Lee KL, Tai YH, Wei PK (2011) Structure effect on sensitivity of gold nanoslits studied by spectral integration method. Plasmonics 6: 483–490
8. Wang LN, Xu BZ, Bai WL, Zhang J (2012) Multiple surface plasmon resonances in compound structure with metallic nanoparticle and nanohole arrays. Plasmonics 7:659–663
9. Wang YH, Wang YQ, Zhang Y, Liu ST (2009) Transmission through metallic array slits with perpendicular cuts. Opt Express 17:5014
10. Yang S, Liu MK, Li JS, Chen X, Xu HX, Zhu QZ, Wang XH, Jin CJ (2011) Extraordinary transmission of three-dimensional crescent-like holes arrays. Plasmonics 7:221–227
11. Lee JW, Yang JK, Sohn IB, Kang C, Kee CS (2013) Folded slot resonator array with efficient terahertz transmission. Opt Commun 293:155–159
12. Chi YM, Chen HL, Lai YS, Chang HM, Liao YC, Cheng CC, Chen SH, Tseng SC, Lin KT (2012) Optimizing surface plasmon resonance effects on finger electrodes to enhance the efficiency of silicon-based solar cells. Energy Environ Sci 6:935–942
13. Lu XC, Zhang WL (2009) Terahertz localized plasmonic properties of subwavelength ring and coaxial geometries. Appl Phys Lett 94: 181106
14. Najiminaini M, Vasefi F, Kaminska B, Carson JJL (2012) Nano-hole array structure with improved surface plasmon energy matching characteristics. Appl Phys Lett 100:043105

15. Sturman B, Podivilov E, Gorkunov M (2011) Optical properties of periodic arrays of subwavelength slits in a perfect metal. Phys Rev B 84:205439
16. Genet C, Ebbesen TW (2007) Light in tiny holes. Nature 445:39
17. Klein Koerkamp KJ, Enoch S, Segerink FB, van Hulst NF, Kuipers L (2004) Strong influence of hole shape on extraordinary transmission through periodic arrays of subwavelength holes. Phys Rev Lett 92: 183901
18. Orbons SM, Roberts A (2006) Resonance and extraordinary transmission in annular aperture arrays. Opt Express 14:12623
19. Gordon R, Brolo AG, McKinnon A, Rajora A, Leathem B, Kavanagh KL (2004) Strong polarization in the optical transmission through elliptical nanohole arrays. Phys Rev Lett 92:037401
20. Degiron A, Ebbesen TW (2005) The role of localized surface plasmon modes in the enhanced transmission of periodic subwavelength apertures. J Opt A Pure Appl Opt 7:S90–S96
21. Xu JJ, Guan P, Kvasnicka P, Gong H, Homola J, Yu QM (2011) Light transmission and surface-enhanced Raman scattering of quasi-3D plasmonic nanostructure arrays with deep and shallow Fabry-Perot nanocavities. J Phys Chem C 115:10996–11002
22. Parsons J, Hendry E, Burrows CP, Auguié B, Sambles JR, Barnes WL (2009) Localized surface-plasmon resonance in periodic nondiffracting metallic nanoparticle and nanohole arrays. Phys Rev B 79:073412
23. Lovera P, Jones D, Corbett B, O'Riordan A (2012) Polarization tunable transmission through plasmonic arrays of elliptical nanopores. Opt Express 20:25325
24. Rodrigo SG, Mahboub O, Degiron A, Genet C, Garcia-Vidal FJ, Martin-Moreno L, Ebbesen TW (2010) Holes with very acute angles: a new paradigm of extraordinary optical transmission through strongly localized modes. Opt Express 18:23691–23697
25. Bao YJ, Peng RW, Shu DJ, Wang M, Lu X, Shao J, Lu W, Ming NB (2008) Role of interference between localized and propagating surface waves on the extraordinary optical transmission through a subwavelength-aperture array. Phys Rev Lett 101:087401
26. Wang CL, Gu JQ, Han JG, Xing QR, Tian Z, Liu F, Chai L, Li YF, Hu ML, Wang QY, Lu XC, Zhang WL (2010) Role of mode coupling on transmission properties of subwavelength composite hole-patch structures. Appl Phys Lett 96:251102
27. Ruan Z, Qiu M (2006) Enhanced transmission through periodic arrays of subwavelength holes: the role of localized waveguide resonances. Phys Rev Lett 96:233901
28. Subramania G, Foteinopoulou S, Brener I (2011) Nonresonant broadband funneling of light via ultrasubwavelength channels. Phys Rev Lett 107:163902
29. Shen HH, Maes B (2012) Enhanced optical transmission through tapered metallic gratings. Appl Phys Lett 100:241104
30. He RJ, Zhou XL, Fu YQ, Zhang YW (2011) Near-field optical experimental investigation of gold nanohole array. Plasmonics 6: 171–176
31. Wang DQ, Yu XL, Yu QM (2012) X-shaped quasi-3D plasmonic nanostructure arrays for enhancing electric field and Raman scattering. Nanotechnology 23:405201–405209
32. Lin L, Roberts A (2011) Light transmission through nanostructured metallic films: coupling between surface waves and localized resonances. Opt Express 19:2626–2633
33. Johnson PB, Christy RW (1972) Optical constants of the noble metals. Phys Rev B 6:4370–4379